Title: Dietary fat and fiber impacts intestinal microbiome resilience to antibiotics and *Clostridoides difficile* infection in mice

Authors: Keith Z. Hazleton[1,2], Casey G. Martin[3], Kathleen L. Arnolds[3], Nichole M. Nusbacher [4], Nancy Moreno-Huizar[4], Michael Armstrong[5], Nichole Reisdorph[5], Catherine A. Lozupone[4]*

Affiliations:

[1] Department of Pediatrics, Section of Gastroenterology, Hepatology and Nutrition. University of Colorado, Denver Anschutz Medical Campus, Aurora, CO USA 80045.

[2]Digestive Health Institute, Children's Hospital Colorado, Aurora, CO USA 80045.

[3] Department of Immunology and Microbiology, University of Colorado, Denver Anschutz Medical Campus, Aurora, CO USA 80045.

[4] Department of Medicine, Division of Biomedical Informatics and Personalized Medicine, University of Colorado, Denver Anschutz Medical Campus, Aurora, CO USA 80045.

[5] Skaggs School of Pharmacy and Pharmaceutical Sciences, University of Colorado Anschutz Medical Campus, Aurora, CO USA 80045.

*To whom correspondence should be addressed: Catherine.lozupone@cuanschutz.edu

One Sentence Summary: High dietary fat promoted mortality in a mouse model of antibiotic-induced *C. difficile* infection and low dietary fiber caused higher microbiome disturbance upon broad-spectum antibiotic exposure, suggesting that diets low in fat and high in fiber may protect against *C. difficile* pathogenesis.

Abstract: *Clostridoides difficile* infection (CDI) is a leading cause of hospital-acquired diarrhea and there has been a steady increase in the number of new infections, emphasizing the importance of novel prevention strategies. Use of broad-spectrum antibiotics and disruption of the intestinal microbiome is one of the most important risk factors of CDI. We used a murine model of antibiotic-induced CDI to investigate the relative contributions of high dietary fat and low dietary fiber on disease pathogenesis. We found that high fat, but not low fiber resulted in increased mortality from CDI (HR 4.95) and increased levels of *C. difficile* toxin production compared to a regular low-fat/high-fiber mouse diet even though we did not observe a significant change in *C. difficile* carriage. The high-fat diet also increased levels of primary bile acids known to be germination factors for *C. difficile* spores. Mice fed low-fat/low-fiber diets did not show increased CDI pathogenesis, but did have a larger antibiotic-induced gut microbiome disturbance compared to mice fed a high-fiber diet, characterized by a greater decrease in alpha diversity. This microbiome disturbance was associated with a loss of secondary bile acids and short chain fatty acids, which are both microbial metabolic products previously shown to protect against CDI. These data suggest that a low-fiber diet contributes to antibiotic-induced dysbiosis, while a high-fat diet promotes CDI pathogenesis. These findings indicate that dietary interventions that increase fiber and decrease fat may be an effective prevention strategy for individuals at high risk of CDI.

Introduction

Clostridoides difficile infection (CDI) is an important cause of morbidity and mortality, with 500,000 cases every year causing 30,000 deaths per year in the US alone *(1)*. Alarmingly, there has been a steady increase in the number of new infections in spite of prevention efforts in hospitals that have focused largely on increased sanitation and antibiotic stewardship *(2)*. These prevention approaches treat CDI as a traditional communicable infection. However, recent data suggests that CDI is often caused by the activation of strains that were already carried in the gut prior to hospital admission and prior to the onset of symptoms rather than by acquisition of a hospital-resident strain *(3)*. Thus, determining strategies to reduce *C. difficile* carriage and attenuate CDI severity is critical.

A complex gut microbiome has been shown to be protective against CDI *(4)*. Broad spectrum antibiotic usage, such as clindamycin, beta-lactams, and fluoroquinolones *(5, 6)* increase risk of CDI as do other illnesses associated with reduced gut microbiome diversity, such as Inflammatory Bowel Diseases *(7)*. Individuals with recurrent CDI (rCDI) typically have microbiomes with greatly reduced complexity and altered compositions *(8-12)*. The gut microbiome provides protection in part through conversion of conjugated primary bile acids, which are excreted by the liver into the intestine where they play a central role in fat digestion, into secondary bile acids. Taurine-conjugated primary bile acids can promote the germination and growth of *C. difficile* spores while secondary bile acids cause germination but arrest the growth of spores *(13)*. Accordingly, prior studies have shown that secondary bile acid producers such as *Clostridium scindens* can protect against CDI in mice *(14)*. Another class of bacterial metabolites that inhibits *C. difficile* are short chain fatty acids (SCFA), which are microbial

63 products of fiber fermentation. SCFAs can directly inhibit *C. difficile* growth *in vitro* and are
64 decreased in individuals with rCDI *(15, 16)*

65 Recent studies conducted in mice have suggested that diet modulation has the potential to
66 be an effective prevention strategy for CDI. Mice treated with broad-spectrum antibiotics and fed
67 diets devoid of microbial accessible carbohydrates (MACs; e.g. soluble fibers such as inulin)
68 showed increased persistence of *C. difficile* colonization consistent with a protective role of
69 SCFAs; inulin supplementation of diets low in MACS lead to rapid clearance of *C. difficile* in
70 this model *(15)*. While dietary fiber content can result in microbial metabolites that are protective
71 against CDI, other diet-influenced metabolites seem to promote the pathogenesis of CDI. For
72 instance, consistent with *C. difficile* being auxotrophic for the amino acid proline, experiments
73 conducted in gnotobiotic mice have supported that mice were protected from *C. difficile*
74 colonization with low-proline diets *(4)*.

75 Given that conjugated primary bile acids play a central role in fat digestion and are a
76 germination factor for *C. difficile* spores, we became interested in investigating a role for dietary
77 fat in CDI pathogenesis. In particular, since prior studies have indicated that the fraction of
78 taurine-conjugated colonic bile acids increase with diets high in saturated fat *(17)*, we
79 hypothesized that a high-fat diet could alter the intestinal bile acid composition and drive
80 pathology in a mouse model of CDI. We further hypothesized that the combination of high fat
81 and low fiber in the diet, as is common in individuals in developed countries, would together
82 promote CDI in mice. We found that high dietary fat content in an antibiotic-induced *C. difficile*
83 model induced high mortality from CDI. A low-fiber diet did not cause mortality but did
84 decrease the resilience of the gut microbiome to antibiotic-induced disturbance, a known risk
85 factor for CDI. Taken together, our results suggest that dietary interventions to increase fiber

and, perhaps more importantly, to decrease fat represent effective prevention strategies for individuals at high risk of CDI.

Results

High dietary fat but not low dietary fiber causes increased mortality and toxin production in murine CDI

To understand the relative effects of dietary fat and fiber on CDI, we used an established murine model of antibiotic-induced CDI *(18)*. Specifically, conventional 6-week-old old female C57-bl6 mice were fed 1 of 3 diets: 1) conventional mouse chow that is low-fat/high-fiber, 2) a purified "Western" diet (WD) that had ~2x the content of fat with increased ratio of saturated-to-unsaturated fat compared to chow and only insoluble cellulose as a source of fiber, and 3) the same purified diet as the WD, but with a lower fat content, similar to chow (low-fat/low-fiber) (Table 1). One week after diet switch, mice were treated with a cocktail of antibiotics in their drinking water for 5 days (kanamycin, gentamicin, colistin, metronidazole and vancomycin) followed by an injection of clindamycin and gavage with *C. difficile* VPI 10463 (Fig. 1A). We conducted 2 sets of experiments. In the first set, the experiments were carried out for up to 21 days past *C. difficile* gavage, allowing us to assay effects on mortality and relate these to fecal microbiome composition. In the second set of experiments, mice were sacrificed at day 3 past *C. difficile* gavage (just prior to the observed onset of mortality in the first experiments), so that bile and SCFA levels could be assessed from the cecum (Fig. 1A).

WD-fed mice showed a marked increase in mortality as compared to chow-fed mice (HR 4.95 CI 1.79-13.72) upon CDI exposure, and significantly higher levels of *C. difficile* toxin B in

the cecum after 3 days of infection (Fig. 1B, C). The low-fat/low-fiber diet-fed mice showed survival and *C. difficile* toxin B levels comparable to the chow-fed mice (Fig. 1B, C). Using qPCR to compare the relative abundance *C. difficile* to overall bacterial load in fecal samples collected 2 days after *C. difficile* challenge, we did not observe any significant differences in *C. difficile* carriage based on diet (Fig. 1D).

Because our WD and low-fat/low-fiber diet differed in sucrose content, we also tested a fourth diet that was low in fat and fiber, but with sucrose equivalent to the WD (Table S1). Sucrose does not appear to play a role in the increased mortality observed in the WD, as 100% survival was observed in mice fed this fourth diet (n = 10, one cage with 5 mice in two separate experiments) and those who received the low-fat/low-fiber/low-sucrose diet.

119 **Table 1**

	Low-fat/High fiber Chow diet	***High-fat/Low-fiber Western diet (WD)***	***Low-fat/Low-fiber diet***
Fat (% kcal) *(% SFA)* *(% MUFA)* *(% PUFA)*	16 *(N/A)*	34.5 *(36.2)* *(41.3)* *(22.5)*	17.2 *(19.5)* *(41.7)* *(38.8)*
Carbohydrates (% kcal) *(Sucrose)*	60 *(0)*	50 *(23.4)*	63.9 *(10.6)*
Protein (%kcal)	24	15.5	18.8
Fiber (g/kg)	137	50 (cellulose)	50 (cellulose)

120

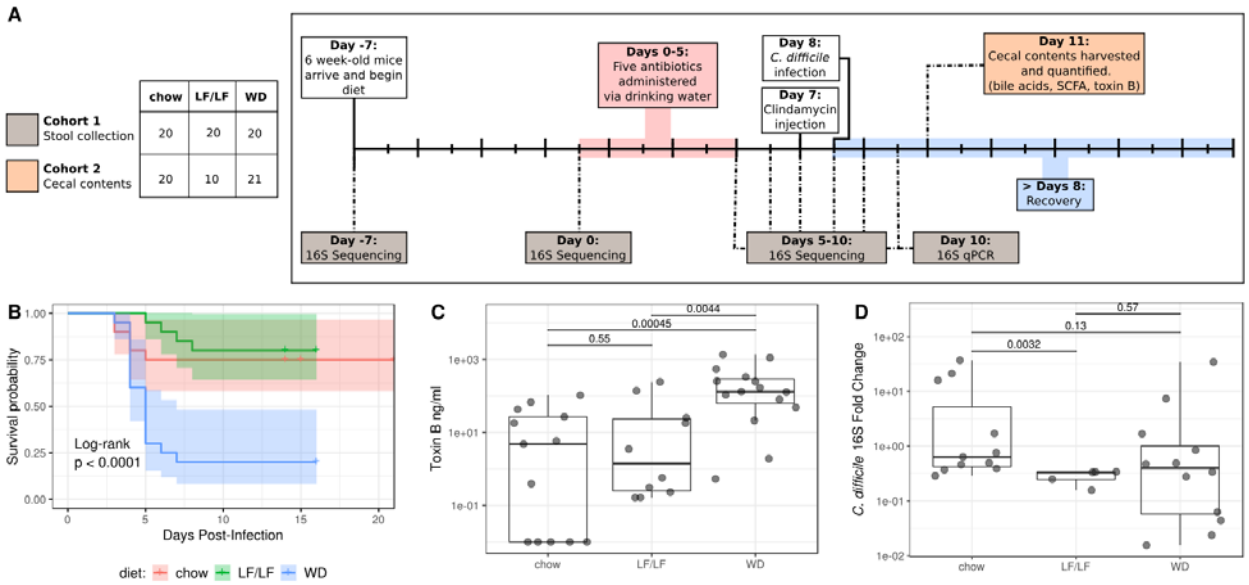

Figure 1: Experimental design of murine model of antibiotic-induced CDI, survival curves and *C. difficile* toxin production and colonization of mice on varying diets. **A)** *C. difficile* challenge experimental design. The figure legend at the left panel indicates the samples sizes for the 2 cohorts. Grey and orange boxes indicate the timepoints at which samples were collected for the respective cohorts **B)** Survival curves on the 3 diets. Both chow and low-fat/low-fiber (LF/LF) diets show increased survival as compared to WD (high-fat/low-fiber). Statistical significance as assessed by log-rank comparison is indicated. **C)** Toxin B levels measured in cecal contents of mice by ELISA (tgcBiomics) at day 3 post infection. Statistical significance was assessed with the Wilcoxon rank-sum test. **(D)** qPCR of *C. difficile* normalized to total 16S from fecal pellets in fecal samples collected 2 days post *C. difficile* challenge, with significance determined by Wilcoxon rank-sum test.

Fiber increases cecal levels of secondary bile acids and butyrate; fat increases taurine-conjugated primary bile acids

To understand the effects of diet modulation on microbial metabolites previously described to modulate *C. difficile* sporulation, growth and activity, we assessed levels of bile acids and SCFAs in aspirated cecal contents that were collected in a separate cohort of 51 mice (chow= 20, WD = 21, low-fat/low-fiber = 10) sacrificed at 3 days post *C. difficile* infection, which is just before mortality typically occurred with the WD diet (Fig. 1A). A total of 17 bile acids including conjugated and unconjugated primary bile acids found in both humans and mice and secondary bile acids, were quantified using HPLC/QTOF using the method described in *(19)* with modifications (see methods). We found that mice fed a WD showed significantly increased levels of taurine-conjugated primary bile acids compared to chow with a trend towards increased level compared to the low-fat/low-fiber diet (Fig 2A, Fig. S1C). The primary unconjugated bile acids (e.g. beta-muricholic acid, cholic acid) did not show a consistent pattern of change based on diet (Fig. S1A) and glycine conjugated bile acids were minimally detectable, which is consistent with mouse metabolism of bile acids strongly favoring taurine conjugation. Finally, the chow-fed mice demonstrated high levels of bacterially-produced secondary bile acids as compared to both WD and low-fat/low-fiber diets (Fig. 2A).

The SCFAs butyrate, acetate and propionate were also quantified in cecal contents 3 days after *C. difficile* infection using gas-chromatography/mass spectrometry (GC/MS). Consistent with SCFAs being microbial fermentation products of dietary fiber, cecal levels of butyrate were reduced in the WD and low-fat/low-fiber diets compared to chow (Fig. 2B). The SCFAs acetate and propionate showed a reduction in the low-fat/low-fiber but not the WD compared to chow Fig. 2B). Interestingly, there was a strong positive correlation between levels of the secondary

bile acid deoxycholate (DCA) and butyrate in both the chow and WD-fed mice, with a markedly increased effect size (slope) in the chow-fed mice (Fig. 2C). For chow-fed mice DCA levels increase by 94.4 pmol/mg wet weight for every 1 mmol/kg increase in butyrate ($p = 5.4 \times 10^{-9}$). Diet alone was not associated with DCA levels ($p = 0.500$), but there was a significant interaction between diet and butyrate; for WD-fed mice DCA levels increase by 18.92 pmol/mg wet weight for every 1 mmol/kg increase in butyrate ($p = 5.1 \times 10^{-5}$). All low-fat/low-fiber samples were omitted from the regression as none of the sample had detectable DCA. Additionally, a single sample from the chow cohort (butyrate = 11.31 mmol/kg, DCA = 342 pmol/mg wet weight) was omitted due to its outsized influence on the regression fit (DFFITs = -12.7).

To explore a direct relationship between microbial metabolites and *C. difficile* pathogenicity, we determined whether any bile acids or SCFAs correlated with *C. difficile* toxin production using linear regression. The model [Toxin B] ~ diet had an adjusted R-squared of 0.1748 and p-value of 0.0131. The only metabolite that was associated with toxin B concentration in univariate analysis was taurocholic acid-3-sulfate (TCA-3-SO4) (Table S2). However, from multivariate analysis it would appear that this association is driven by collinearity of TCA-3-SO4 and Toxin B concentrations with respect to diet (Fig. S2). Addition of other individual metabolites to the regression model with diet (e.g. Toxin B ~ metabolite + diet or Toxin B ~ metabolite + diet + diet*metabolite) did not improve the regression model, suggesting that dietary control of toxin production is independent of the metabolites we interrogated.

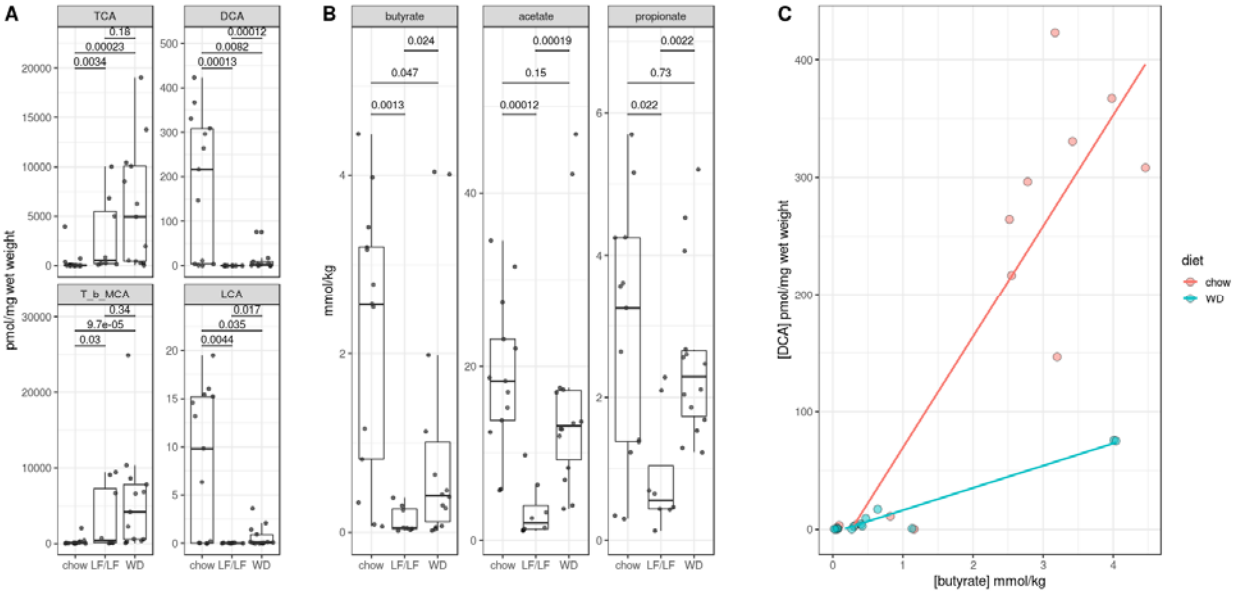

Figure 2: Metabolite changes in cecal contents of infected mice 3 days post *C. difficile* infection. **(A)** Cecal levels of taurine-conjugated primary bile acids (left column) and bacterially-produced secondary bile acids (second column) across diets. TCA= Taurocholic acid; T-b-MCA=Tauro-b-muricholic acid; DC=Deoxycholic acid; LCA=Lithocholic acid. **(B)** Cecal short chain fatty acid levels across diets. P-values were determined using the Wilcoxon rank-sum statistical test. **(C)** Multiple linear regression of DCA levels as a function of butyrate and diet. Model = DCA ~ butyrate + diet + butyrate*diet. R-squared 0.855 p <0.0001. Low-fat/low-fiber samples were excluded from analysis since there was no detectable DCA.

Dietary fiber increases homogeneity of response, resilience and alpha-diversity of the gut microbiome after challenge with antibiotics and CDI

We next sought to understand how the composition of the fecal microbiome was affected by diet during the course of antibiotic treatment and infection with *C. difficile* (Fig. 1A). Fecal pellets were collected upon arrival prior to diet change (Day -7), just prior to the start of oral antibiotic delivery (Day 0), after 5 days of oral antibiotics (Day 5), and daily through Day 10, which captured before and after the clindamycin injection given on day 7 and *C. difficile* gavage on Day 8 (Fig. 1A). Collected samples were subjected to 16S ribosomal RNA (rRNA) amplicon sequencing targeting the V4 region of rRNA on the MiSeq platform.

Principle coordinate analysis (PCoA) plots of a weighted UniFrac distance matrix suggested that mice fed either low-fiber diet had decreased resilience and a less homogeneous response to antibiotic challenge and CDI as compared to chow-fed mice. Mice fed either low-fiber diet showed greater divergence across PC1 upon antibiotic exposure than chow-fed mice, higher spread across mice in the same diet group, and less recovery towards their baseline after antibiotics (Fig. 3A). We quantified resilience by comparing the pairwise weighted UniFrac distances of mice across the experiment to baseline microbiota of their respective diet cohort at Day 0 (7 days post-diet change and pre-oral antibiotics; Fig. 3B). Chow-fed mice had significantly smaller weighted UniFrac distances from their baselines than the other groups at Day 5 (post 5 days antibiotic challenge) that persisted through Day 10 despite some convergence after clindamycin injection (Day 8) (Fig. 3B). By Day 9, chow-fed mice again displayed higher microbiome resilience than both low-fiber groups. We also assessed the homogeneity of response to a disturbance among mice in the same diet group. As an example, low homogeneity would occur if the mice within a diet group showed high variability in the degree to which their

gut microbiome changed upon antibiotic exposure. We quantified this as the median pairwise weighted UniFrac distance for comparisons within samples collected at the same time point from mice fed the same diet (Fig. 3C). Both low-fiber diets showed much lower homogeneity of gut microbiome compositional response to antibiotic challenge, particularly to the 5 day treatment with oral antibiotics (Day 5), compared to chow-fed mice (Fig. 3C).

Similar patterns were seen when evaluating changes in alpha-diversity across the experiment between each diet cohort. Figure 4 shows changes in phylogenetic entropy, which is a measure of alpha diversity that considers species richness, evenness, and distinctness *(20)*. The phylogenetic entropy of the WD-fed mice was lower than chow-fed mice after diet change and this difference became more pronounced upon oral antibiotics and remained so through the rest of the experimental timeline (Fig. 4). Interestingly, the phylogenetic entropy of the low-fat/low-fiber diet-fed mice remained equivalent to the chow-fed cohort with diet change but decreased to the same level as the WD with antibiotic treatment (Fig. 4).

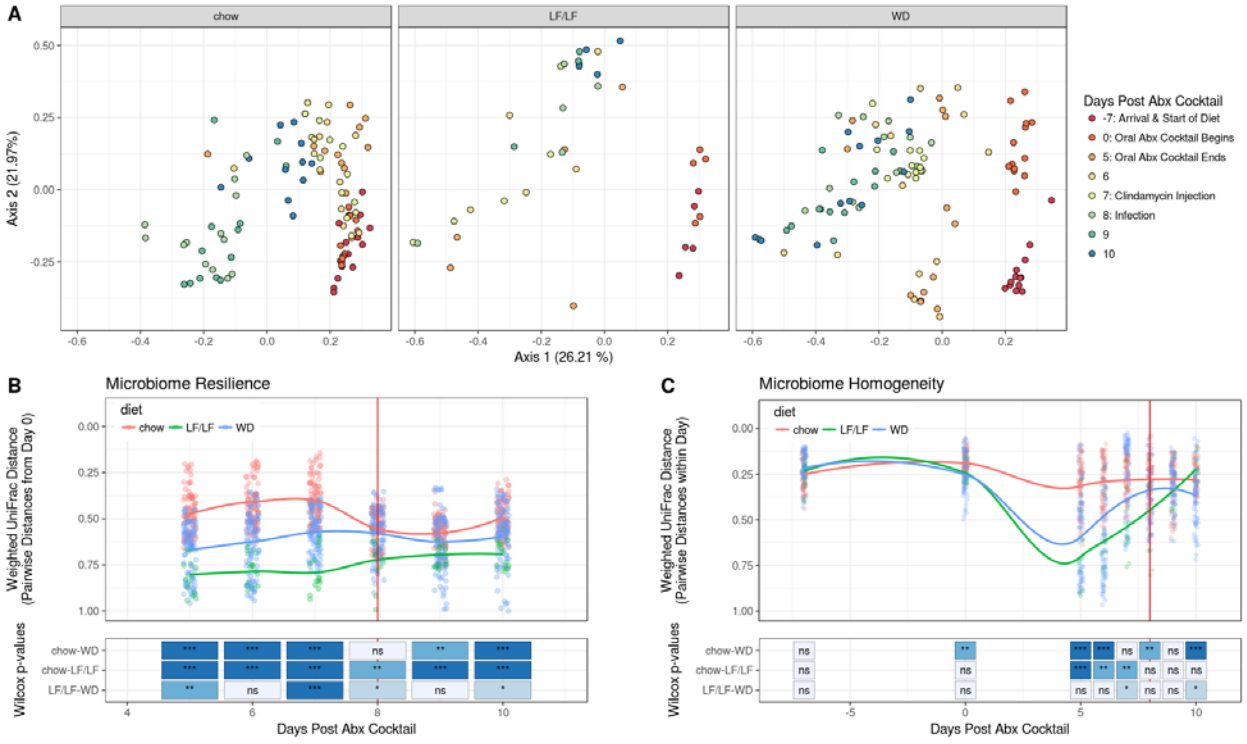

Figure 3: Beta diversity plots of fecal microbiome by diet during antibiotic treatment and infection with *C. difficile*. Vertical red lines in panels B and C designate the day of *C. difficile* infection. (A) Weighted UniFrac PCoA plots of all samples with each diet highlighted in separate panels. (B) Resilience of microbiome composition assessed by within-mouse pairwise weighted UniFrac distances between Day 0 (7 days post diet switch and prior to oral antibiotics) and later time points and (C) Longitudinal plot of microbiome turnover homogeneity as plotted by intra-time point pairwise Weighted UniFrac distances within diet groups. Trend lines were fit using local polynomial regression.

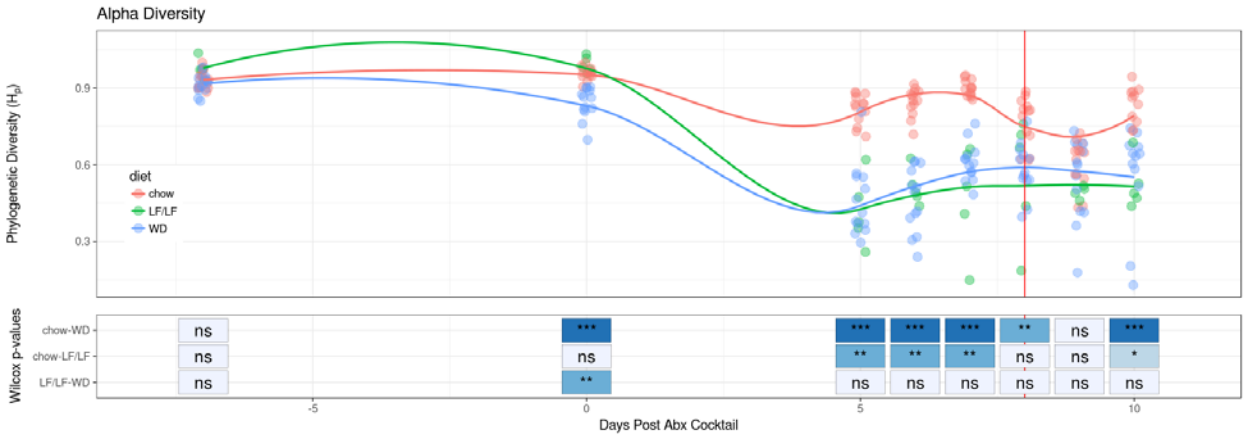

Figure 4: Alpha-diversity (phylogenetic entropy) of the fecal microbiome during murine CDI model. Data for each individual mouse is plotted as well as the fitted local polynomial regression for each diet group. Significant differences between groups are noted as calculated with the Wilcoxon rank-sum test. ***: p<0.001. **: p<0.01, *: p<0.05 ns= non significant.

Dietary fiber influences colonization patterns of facultative anaerobes and of secondary bile acid and SCFA-producing bacteria

Low-diversity dysbiosis is a state of disturbance that is often characterized not only by low alpha-diversity, but also by an increased ratio of facultative to strict anaerobes *(21)*. Low-diversity dysbiosis is associated with a number of diseases including rCDI *(21)*. We sought to investigate whether high dietary fat and low dietary fiber influenced if the microbiome developed a compositional state characterized by high levels of facultative anaerobe colonization and lower levels of strict anaerobes. Since Lactobacilliales and Enterobacteriales contain many important intestinal facultative anaerobes and most members of Clostridiales are strict anaerobes and include key butyrate and secondary bile acid producers, we plotted the relative abundances of these orders over the course of the experiment (Fig. 5A). All mice had decreases in the relative abundance of Clostridiales in their fecal microbiome with oral antibiotics; however, mice fed a chow diet were able to maintain a Clostridiales population while both low-fiber diets saw near-complete elimination of these taxa (chow-WD $p<0.01$ for days 0 through 9 and $p<0.05$ on day 10, Fig. S3). Conversely, mice fed either low-fiber diet had a large bloom of Lactobacilliales after oral antibiotic treatment that was not observed in the chow-fed mice (chow-WD $p<0.001$ and chow-low-fat/low-fiber $p<0.05$). Lastly, all 3 diet groups had a large increase in Enterobacteriales in their fecal microbiome following antibiotics; however, the low-fat/low-fiber and chow groups showed earlier decrease than WD mice (chow-WD $p<0.01$ and $p<0.05$ at days 9 and 10 respectively, Fig. S3). Comparisons of the low-fat/low-fiber diet were limited due to smaller sample size ($n = 5$ vs. $n = 13$ for chow and WD).

We also used PICRUSt *(22)* to predict metagenomes using our 16S rRNA data 1) to investigate trends in the prevalence of key genes in secondary bile and butyrate production over

the course of our experimental timeline and 2) to predict which bacterial taxa were contributing these genes. Because BaiA, BaiB, and BaiCD are not available in PICRUSt2's set of predicted genes, we only used the genes for BaiH (KEGG ID: K15873) and BaiI (KEGG ID; K15874), which are both genes in the Bai operon *(23)*, to assess genomic potential for secondary bile acid metabolism. Acetoacetate co-A transferase (*but*; K01034) and Butyrate Kinase (*buk*; KEGG ID: K00929), which are the main pathways for fermentative production of butyrate in the gut microbiome *(24)*, were used to assess butyrate production potential. Plotting these genes/pathways over time reveals a significant effect of fiber on their abundance and response to antibiotics (Fig. 5C). Although all diet groups showed a marked decrease in bile acid genes with oral antibiotics, only the chow-fed mice displayed a recovery of bile acids genes, though the source of these genes switched from Lachnospiraceae UCG-006 to Blautia. This result is consistent with our observation of higher cecal levels of secondary bile acids in chow-fed mice compared to mice fed either low-fiber diets at 3 days post *C. difficile* gavage (Fig. 2A).

Fiber also influenced the butyrate coding capacity observed between diet groups. Chow-fed mice showed minimal change in the abundance of both the *but* and *buk* genes for fermentative butyrate production during the time course while the WD mice had a decrease of 5 orders of magnitude (Fig 5D). The low-fat/low-fiber mice showed an intermediate phenotype with the resilience of the butyrate pathway being mostly attributed to a butyrate kinase dependent pathway. The results for *but* and not *buk* however are consistent with our measurements of cecal butyrate levels in these mice 3 days post *C. difficile* gavage (Fig. 2B). This is consistent with *but* being regarded to be a more important source of butyrate in the intestine *(25)*.

Since we had observed a strong positive correlation between cecal levels of butyrate and the secondary bile acid DCA in our mass spectrometry data (Fig. 2C), we also determined

289 whether there was a relationship between butyrate and secondary bile acid coding capacity. We
290 found a highly significant association ($p = 3.6x10^{-5}$), with secondary bile acid producing genes
291 only predicted to be present in samples that also had high predicted levels of butyrate producing
292 genes (Fig. 5B).

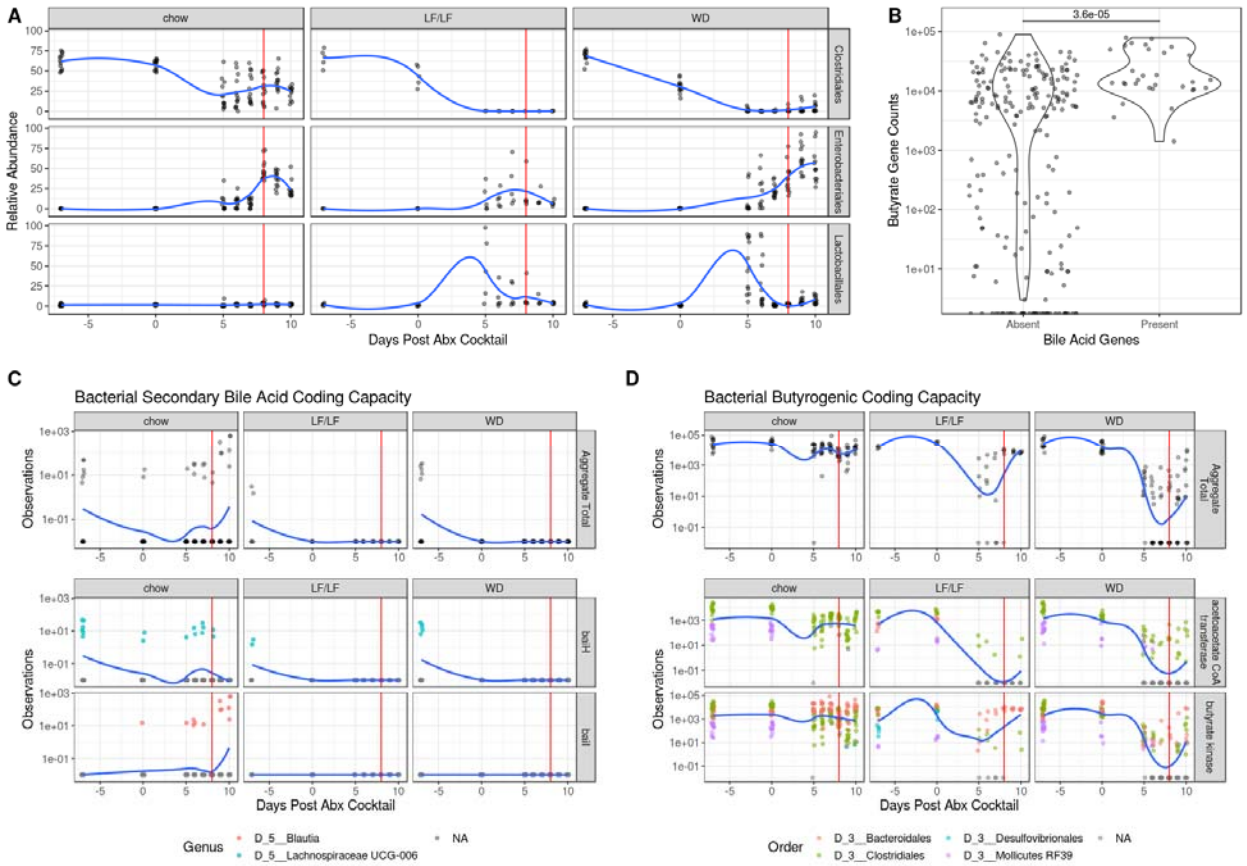

Figure 5: Changes in key taxa, and secondary bile acid and butyrate coding capacity during the CDI protocol. The vertical red line in (A), (C) and (D) represent day of infection with *C. difficile*. All trend lines were fit using local polynomial regression. **(A)** Relative abundance of key bacterial orders during antibiotic treatment and infection. Clostridiales are strict anaerobes while Enterobacteriales and Lactobacilliales are facultative anaerobes. **(B)** Violin plots of abundance of butyrate genes from PICRUSt analysis binned by presence of secondary bile acid producing genes (Wilcoxon $p<0.001$). **(C)** Time course of coding capacity of secondary bile acid genes. The top row shows the total capacity of each sample (BaiH and BaiI) while the bottom two rows show specific taxa contributions of key genes in the Bai operon. **(D)** Time course of coding capacity of butyrate producing genes by diet. The top row shows the total capacity as measured

304 by *but* and *buk* genes while the bottom two rows show specific taxa contributions of *but* and *buk*

305 specifically. Taxa with mean relative abundance < 0.01% were filtered from the analysis.

306

Discussion

Clostridioides difficile infection is a grave and growing health threat. Current strategies to limit its spread have focused on sanitation and antibiotic stewardship, however incidence has continued to rise *in spite* of these efforts, highlighting the need for new treatment and prevention strategies *(2)*. Because of the ubiquity of *C. difficile* spores in the environment, focusing on ways to increase the resilience of the host to colonization is one important prevention strategy. However, modulation of host factors that influence virulence of *C. difficile* already present in the gut is also a key aspect of prevention, as CDI is often caused by *C. difficile* that is already residing in the gut before the onset of symptomatic CDI rather than acquisition of a new infection *(3)*.

A growing body of evidence points to dietary intervention as a promising new approach to prevent CDI colonization *(4, 15)*. One recent study showed that a diet poor in proline (an essential amino acid for *C. difficile* growth) prevented *C. difficile* carriage *(4)*. Another study demonstrated that mice fed a diet deficient in MACs (e.g. soluble fiber, resistant starches) had persistent *C. difficile* shedding and that there was a resolution of colonization with the reintroduction of inulin or other MACs *(15)*. Although these papers both showed a strong effect of dietary factors on *C. difficile* colonization, neither study observed the high levels of mortality that we observed here with a high-fat/low-fiber WD. This is consistent with our findings that a low-fat/low-fiber diet did not increase mortality in our antibiotic induced CDI murine model, and suggests a particularly high influence of dietary fat on CDI disease severity. This is further supported by the fact that *C. difficile* abundance 2 days post *C. difficile* challenge, as quantified by strain-specific qPCR, was not significantly influenced by diet, suggesting that in an acute infection model, *C. difficile* blooms regardless of diet, and that increased disease severity is due

to dietary fat activating toxin production and not from increased *C. difficile* carriage. Furthermore, although new data has suggested that novel speciation of *C. difficile* may be selecting for strains that show increased sporulation and host colonization capacity with sugar (glucose or fructose) *(26)*, this work, conducted with a hyper-virulent *C. difficile* strain (VPI 10463), did not show differences in mortality from CDI in low-fat/low-fiber diets with different amounts of sucrose.

Evidence to suggest that a high-fat/low-fiber western diet could have a more profound effect on CDI was first presented over 20 years ago. In experiments designed to study the atherogenic properties of a Western diet in Syrian hamsters, significant mortality from CDI was observed in hamsters fed a high-fat/low-fiber pro-atherogenic diet and not a typical high-fiber/low-fat hamster diet *(27, 28)*. Our work confirms the same effect of a WD in an antibiotic-induced murine CDI model.

Differences in host bile acid production and microbial bile acid metabolism is one potential mechanism of high-fat diet induced modulation of CDI severity. *In vitro* experiments have shown that the primary bile acid taurocholate is a potent *C. difficile* germination and growth factor *(13)*. We found that mice fed a high-fat/low-fiber WD had higher cecal levels of primary taurine-conjugated bile acids compared to the two low-fat diets tested. This is consistent with a prior study that found that IL10-deficient mice fed a diet high in saturated fat, had an increased proportion of taurine-conjugated bile acids compared to standard chow and a diet high in poly-unsaturated fats *(17)*. However, in our current study multivariate regression did not correlate any species of bile acid with toxin B concentration. This suggests that dietary fat may directly modulate *C. difficile* Toxin B production or act through a non-bile acid dependent pathway to promote CDI in our model.

353 We also sought to explore a role for secondary bile acids in phenotypes observed in diet-
354 induced CDI. *In vitro* experiments have shown that the bacterially produced secondary bile acids
355 deoxycholate and lithocholate caused germination followed by growth arrest of *C. difficile (13).*
356 In line with these effects, reduced prevalence of the secondary bile acid producer, *Clostridium*
357 *scindens* in the fecal microbiome has been associated with high incidence of CDI in both humans
358 and in experimental mouse models, and gavaging mice with *C. scindens* protected against CDI
359 and restored intestinal secondary bile acid levels *(14).* We observed that chow-fed mice had high
360 levels of secondary bile acids compared to both WD and low-fat/low-fiber diets. Functional
361 interrogation of the microbiome using PICRUSt suggests that this might be due to a lack of
362 recovery of secondary bile acid producing bacteria following antibiotic disturbance in both low-
363 fiber diet contexts. However, mice fed the low-fat/low-fiber diet did not demonstrate the
364 increased mortality or high *C. difficile* toxin production observed in the WD despite a lack of
365 secondary bile acids, suggesting that the loss of secondary bile acid producing bacteria were not
366 an important mechanism for the increased mortality and *C. difficile* toxin production observed
367 with a WD.

368 While these data show that a high-fat diet increases *C. difficile* toxin production and
369 mortality in a mouse model of CDI, we did not explore how the composition of fat influences
370 these factors. Our WD composition represents a typical diet in the United States based on
371 population survey data and it has 34.5% of calories from fat, with a roughly equivalent
372 contributions of saturated (~36%), mono-unsaturdated fats (41%) and a lower contribution from
373 poly-unsaturated fats (~21%). In the low-fat/low-fiber diet, these contrubtions are reversed
374 (saturated fat ~19% and poly-unsaturated fat ~39%). Further studies to determine if total fat
375 intake or specific types of fat drive our observed phenotype are needed.

Our data suggests that dietary fiber is critical for the resilience and homogeneity of response of the gut microbiome after perturbation. In both cohorts of mice fed fiber-deficient diets, the gut microbiome was significantly more variable and slower to recover to baseline after perturbation. By supplying the gut with a preferred fuel (fiber) for species associated with health (e.g. strict anaerobes), the community is able to resist antibiotic induced changes and reconstitute more quickly once the pressure of antibiotic treatment has been removed. This finding is consistent with a recent study that showed that fiber supplementation in mice lead to a reduced disruption of the gut microbiome to disturbance from amoxicillin, and that this was linked with upregulation of polysaccharide utilization by *Bacteroides thetaiotaomicron*, an intestinal commensal that individually became less susceptible to amoxicillin in the presence of dietary fiber *(29)*.

This increased resilience of gut microbiome composition to antibiotic disturbance was also reflected through levels of the bacterially produced metabolites that we measured. Neither low-fiber diet was able to maintain butyrate or secondary bile acid production following perturbation. Based on the correlation between butyrate and DCA concentrations, we speculate that the lack of butyrate leads to increased luminal oxygen concentrations that are unsuitable for *Clostridium scindens* and other secondary bile acid producers. Prior work has shown that aerobic metabolism of butyrate by intestinal epithelial cells is a key driver of intestinal hypoxia *(30)*. That there may be increased luminal oxygen concentrations in the low fiber diets is consistent with our observation of a bloom in Lactobacillales order, which is entirely composed of facultative anaerobes, after oral antibiotic challenge in both low-fiber diets but not chow.

While our data do not suggest a role for fiber in protection against mortality from CDI in this mouse model, it would be short-sighted to dismiss the beneficial role of fiber in maintaining

399 a healthy gut microbiome and resistance to CDI. Our model utilized a rather short-term diet
400 change and an intense antibiotic regimen that may not correlate well with human circumstances.
401 We also did not explore diets high in fat and high in fiber, where it is possible that increased
402 microbiome resilience to antibiotics due to fiber may protect from the detrimental effects of fat.
403 As discussed above, a fiber-deficient diet has been shown to hinder clearance of *C. difficile* after
404 challenge *(15)*. This is particularly relevant in a clinical context as recent studies of both
405 pediatric and adult oncology patients have shown asymptomatic colonization rates with *C.*
406 *difficile* of ~30% and ~10%, respectively *(3, 31)*. Further, in pediatric patients it was
407 demonstrated that the vast majority of "hospital-acquired" CDI may be caused by a strain of *C.*
408 *difficile* that is present at admission rather than a strain acquired during the patient stay *(3)*.
409 Our data along with recently published findings investigating dietary fiber *(15)* and
410 dietary proline *(4)* intake provides a compelling case that diet should be increasingly targeted as
411 a prevention and treatment modality for CDI. High-risk populations such as adult and pediatric
412 oncology patients may benefit from decreased *C. difficile* colonization through increased fiber
413 intake. For patients with active infection, limiting fat intake could decrease disease severity
414 while maintaining enteral nutrition.

415 **Materials and Methods**

416 Murine model of CDI: Mice were infected using a widely used murine CDI model *(18)*
417 with minor modifications. Briefly, 6-week-old female C57BL/6 mice from Taconic Bioscience
418 (Rensselaer, NY) arrived at University of Colorado on Day -7 of the experiment. Within 24
419 hours, mouse feed was changed to one of three diets: standard chow, high-fat/low-fiber (Western
420 Diet), or low-fat/low-fiber diet (all groups n=20). After seven days of the new diet, we placed
421 mice on a five-antibiotic cocktail (kanamycin (0.4 mg/ml), gentamicin (0.035 mg/ml), colistin

(850 U/ml), metronidazole (0.215 mg/ml), and vancomycin (0.045 mg/ml)) in their drinking water. Antibiotics were removed for 48 hours, after which we administered an intraperitoneal injection of clindamycin in normal saline (10 mg/kg body weight). Twenty-four hours after injection, we gavaged mice with $1.75x10^5$ cfu of *C. difficile* VPI 10463. We weighed mice daily after removal of oral antibiotics and they were euthanized if they lost >15% of body weight or were moribund. Fecal pellets were collected at arrival (Day -7), after diet change and prior to oral antibiotics (Day 0) and then daily after removal of oral antibiotics (Day 5-10). In a separate experiment, we performed the same experimental protocol on 51 mice (chow = 20, low-fat/low-fiber = 10, WD = 21), but we sacrificed the mice 72 hours after infection and collected cecal contents for short chain fatty acid, bile acid and toxin quantification. All mouse experiments were approved by the Institutional Animal Care and Use Committee and complied with their guidelines and NIH Guide for the Care and Use of Laboratory Animals (IACUC protocol #00249)

DNA Extraction and Sequencing: Total genomic DNA was extracted from fecal pellets from a subset of the mice in cohort 1 (chow = 13 mice from four separate cages over two experiments, WD = 13 mice from four separate cages over two experiments, low-fat/low-fiber = 5 mice from two cages over two experiments) using the DNeasy PowerSoil Kit (Qiagen, Germantown, MD). Modifications to the standard protocol included a 10 minute incubation at 65°C immediately following the addition of the lysis buffer and the use of a bead mill homogenizer at 4.5 m/s for 1 min. The V4 variable region of the 16S rDNA gene was targeted for sequencing (515F: GTGCCAGCMGCCGCGGTAA, 806R: GGACTACHVGGGTWTCTAAT). The target DNA was amplified using HotMaster Mix (Quantabio Beverly, MA). Construction of primers and amplification procedures follow the

Earth Microbiome Project guidelines (www.earthmicrobiome.org) *(32)*. Amplified DNA was quantified in a PicoGreen (ThermoFisher Scientfic) assay and equal quantities of DNA from each sample was pooled. The pooled DNA was sequenced using a V2 2x250 kit on the Illumina MiSeq platform (San Diego, CA) at the University of Colorado Anschutz Medical Campus Genomics and Microarray Core facility.

Sequence Data Analysis: Raw paired-end FASTQ files were processed with QIIME 2 version 2018.8 *(33)*. Denoising was performed with DADA2 *(34)*, a phylogenetic tree was built using sepp *(35)* and taxonomy was assigned to amplicon sequence variants (ASVs) using the RDP Classifier *(36)* trained on the Silva version 132 taxonomic database *(37, 38)* using QIIME 2. The data was rarefied at 5,746 sequences per sample. Alpha-diversity was measured by phylogenetic entropy *(20)* and beta-diversity was determined by weighted UniFrac distances *(39)*. PCoA of weighted UniFrac plots were constructed using QIIME 2. Metagenomes were imputed from 16S ASVs using PICRUSt2's default pipeline for stratified genome contributions *(22)*. Low abundance taxa (<0.01% mean relative abundance) were filtered for analysis of the butyrogenic coding capacity. Software was installed using Anaconda *(40)*and analysis was performed on the Fiji compute cluster at the University of Colorado Boulder BioFrontiers Institute.

***C. difficile* and 16S Quantitative PCR:** qPCR was performed on extracted DNA from fecal pellets from cohort 1 on day 10 of the experiment with primers targeting the V4 region of 16S rRNA (see above) and strain specific *C. difficile* VPI 10463 *(41)*. The qPCR was prepared using Kapa SYBR Fast qPCR master mix (Roche Wilmington, MA) and completed on the CFX96 platform (BioRad Hercules, CA).

SCFA quantification: The SCFAs butyrate, propionate, and acetate were analyzed by stable isotope GC/MS as previously described *(42)*. Briefly, cecal samples were collected directly into pre-weighed, sterile Eppendorf tubes and flash frozen at −80°C until processing. Samples were then subject to an alkylation procedure in which sample and alkylating reagent were added, vortexed for 1 min, and incubated at 60°C for 25 min. Following cooling and addition of n-hexane to allow for separation, 170 µL of the organic phase was transferred to an auto sampler vial and analyzed by GC/MS. Results were quantified in reference to the stable isotope standard and normalized to sample weight.

Bile acids quantification: *Reagents:* LC/MS grade methanol, acetonitrile, and isopropanol were obtained from Fisher Scientific (Fairlawn, New Jersey). HPLC grade water was obtained from Burdick and Jackson (Morristown, New Jersey). Acetic acid, cholic acid, chenodeoxycholic acid, lithocholic acid, glycolithocholic acid, glycodeoxycholic acid, glycochenodeoxycholic acid, taurocholic acid and deoxycholic acid were obtained from Sigma Aldrich (St. Louis, Missouri). Glycolithocholic acid, taurodeoxycholic acid, taurochenodeoxycholic acid, taurolithocholic acid, alpha-muricholic acid and beta-muricholic acid were obtained from Cayman Chemical (Ann Arbor, Michigan). Chenodeoxycholic acid-d4 and glycochenodeoxycholic acid-d4 were obtained from Cambridge Isotope labs (Tewksberry, Massachusetts).

Standards preparation: An internal standard containing 21 µM of chenodeoxycholic acid-d4 and 21 µM of glycochenodeoxycholic acid–d4 was prepared in 100% methanol. A combined stock of all bile acid standards was prepared at 0.5mM in 100% methanol. Calibration working standards were then prepared by diluting the combined stock over a range of 0.05 µM-50 µM in methanol. A 20 µL aliquot of each calibration working standard was added to 120 µL

of methanol, 50 µL of water and 10 µL of internal standard (200 µL total) to create 10 calibration standards across a calibration range of 0.005 µM-5 µM.

Sample preparation: Fecal samples were prepared using the method described by Sarafian et al *(19)* with modifications. Briefly, 15-30mg of fecal sample were weighed in a tared microcentrifuge tube and the weight was recorded. 140 µL of methanol, 15-30 µL of water and 10 µL of internal standard were added. The sample was vortexed for 5 seconds, and then incubated in a -20°C freezer for 20 minutes. The sample was then centrifuged at 6000RPM for 15 minutes at 4°C. 185-200 µL of the supernatant was transferred to an RSA autosampler vial (Microsolv Technology Corporation, Leland, NC) for immediate analysis or frozen at -70°C until analysis.

High performance liquid chromatography/quadrupole time-of-flight mass spectrometry (HPLC/QTOF): HPLC/QTOF mass spectrometry was performed using the method described by Sarafian et al *(19)* with modifications. Separation of bile acids was performed on a 1290 series HPLC from Agilent (Santa Clara, CA) using an Agilent SB-C18 2.1X100mm 1.8 µm column with a 2.1X 5mm 1.8um guard column. Buffer A consisted of 90:10 water:acetonitrile with 1mM ammonium acetate adjusted to pH=4 with acetic acid, and buffer B consisted of 50:50 acetonitrile:isopropanol. 10 µL of the extracted sample was analyzed using the following gradient at a flow rate of 0.6mls/min: Starting composition=10%B, linear gradient from 10-35% B from 0.1-9.25 minutes, 35-85% B from 9.25-11.5 minutes at 0.65mls/min, 85-100% B from 11.5-11.8 minutes at 0.8mls/min, hold at 100% B from 11.8-12.4 minutes at 1.0ml/min, 100-55% B from 12.4-12.5 minutes 0.85mls/min, followed by re-equilibration at 10%B from 12.5-15 minutes. The column temperature was held at 60°C for the entire gradient.

Mass spectrometric analysis was performed on an Agilent 6520 quadrupole time of flight mass spectrometer in negative ionization mode. The drying gas was 300°C at a flow rate of 12mls/min. The nebulizer pressure was 30psi. The capillary voltage was 4000V. Fragmentor voltage was 200V. Spectra were acquired in the mass range of 50-1700m/z with a scan rate of 2 spectra/sec.

Retention time and m/z for each bile acid was determined by injecting authentic standards individually. All of the bile acids produced a prominent $[M-H]^-$ ion with negative ionization. The observed retention time and m/z was then used to create a quantitation method. Calibration curves for each calibrated bile acid were constructed using Masshunter Quantitative Analysis software (Aligent Technologies). Bile acid results for feces in pmol/mg were then quantitated using the following calculation:

$$\text{Concentration in pmol/mg} = \frac{(X_s)(V_t)(D)}{(V_i)(W_s)}$$

X_s =pmol on column

V_t =Total volume of concentrated extract (in µL)

D =Dilution factor if sample was extracted before analysis. If no dilution D=1

V_i =Volume of extract injected (in µL)

W_s =Weight of sample extracted in mg

***C. difficile* toxin B quantification:** Toxin B concentration was determined in cecal samples from day 3 of infection by comparison to a standard curve using ELISA (tgcBiomics,

Germany). For samples that were too small to weigh accurately, a mass of 5 mg was assigned for concentration calculation. This mass was selected as it was the lowest weight that could be accurately determined.

Statistics: Statistical analyses were performed in R (version 3.4.3 "Kite-Eating Tree"). Data were preprocessed using the "tidyverse" suite *(43)*. We used "survminer" and "survival" libraries to analyze mouse survival *(44, 45)*. All other data were plotted using "ggplot2", "ggsignif", and "cowplot" *(46-48)*.

Supplementary Materials

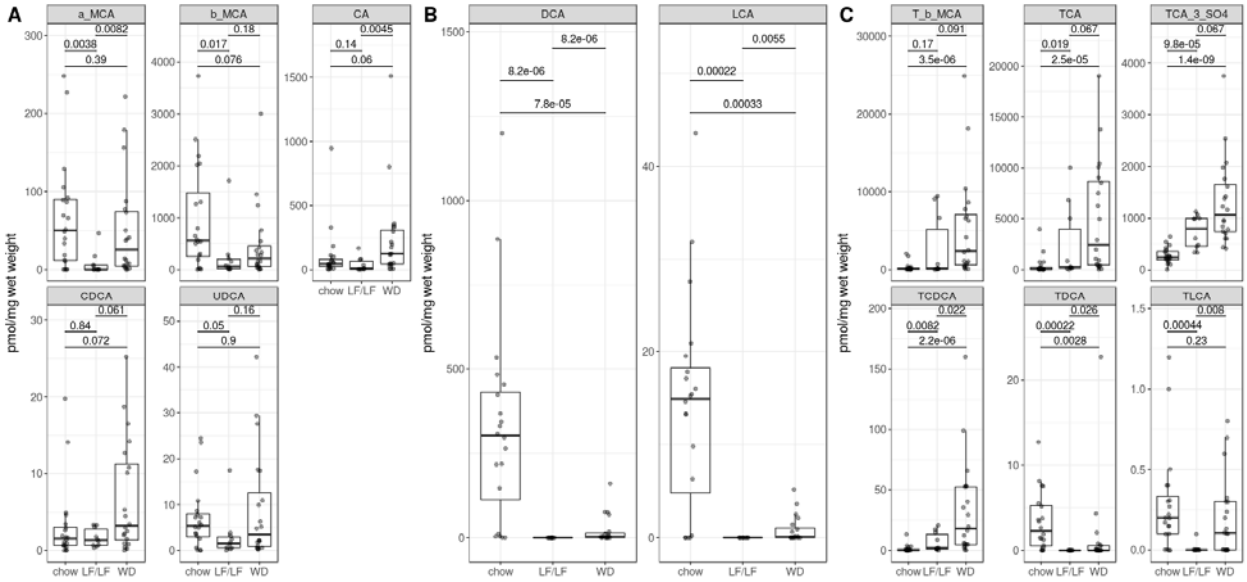

Figure S1. Cecal bile acid levels by diet. Unconjugated primary bile acids (A), secondary bile acid (B) and taurine-conjugated bile acids (C). Glycine conjugated bile acids were omitted due to very low concentrations. a_MCA (alpha muricholic acid); b_MCA (beta muricholic acid); CA (cholic acid); CDCA (chenodeoxycholic acid) ;UDCA (ursodeoxycholic acid); DCA (deoxycholic acid); LCA (lithocholic acid); T_b_MCA (tauro-beta muricholic acid); TCA (taurocholic acid); TCA_3_SO4 (taurocholic acid 3-sulfate); TCDCA (taurochenodeoxycholic acid); TDCA (taurodeoxycholic acid); TLCA (taurolithocholic acid).

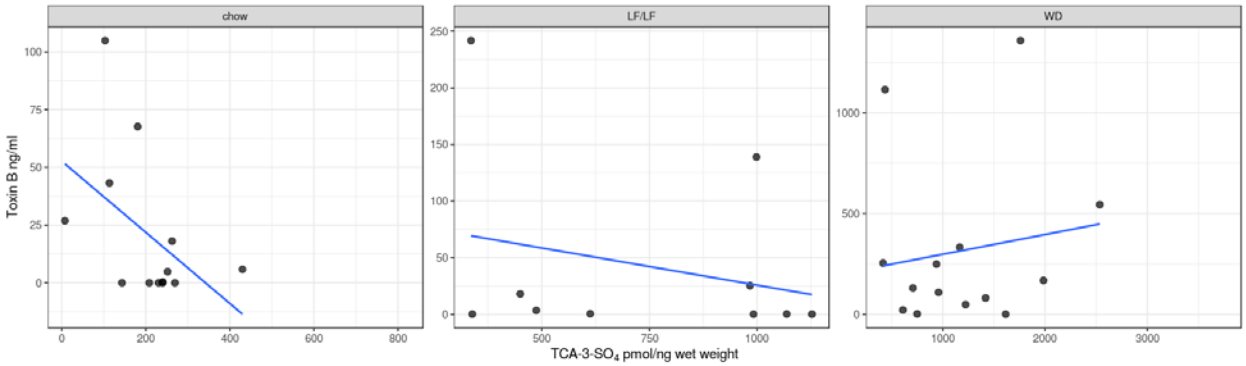

550

551 **Figure S2.** Toxin B ~ TCA-3-SO4 correlations by diet. Multivariate regression was performed

552 allowing for an interaction between toxin B and diet.

553

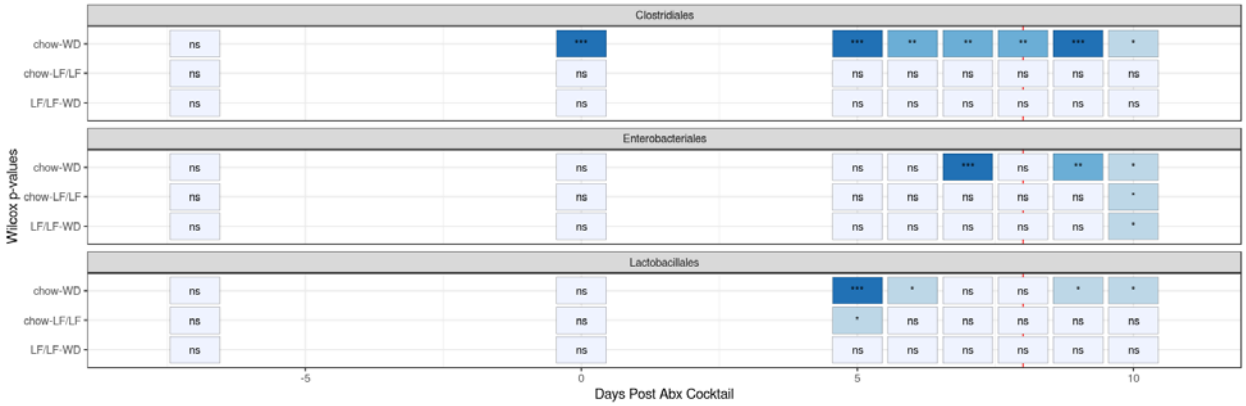

554

555 **Figure S3:** Statistical summary of relative abundances of key taxa from Figure 5a. Significant

556 differences between groups are noted as calculated with the Wilcoxon rank-sum test. ***:

557 p<0.001. **: p<0.01, *: p<0.05, ns= non significant.

558 Table. S1. Composition of low-fat/low-fiber/high-sucrose diet

	Low-fat/Low-fiber/High-Sucrose
Fat (% kcal) *(% SFA)* *(% MUFA)* *(% PUFA)*	17.0 *(19.5)* *(41.7)* *(38.8)*
Carbohydrates (% kcal) *(Sucrose)*	64.5 *(26.7)*
Protein (%kcal)	18.6
Fiber (g/kg)	50 (cellulose)

559

560

561 Table S2. Correlations between *C. difficile* toxin B and metabolites

Formula = toxin_B ~ x		R-squared	p-value
~ diet		0.1748	0.0131
	Bile acids		
		R-squared	p-value
TCA_3_SO4	~ metab	0.1151	0.0227
	~ metab + diet	0.1701	0.0273
	~ metab + diet + metab*diet	0.1748	0.0131
T_b_MCA	~ metab	-0.0156	0.5078
	~ metab + diet	0.1739	0.0254
	~ metab + diet + metab*diet	0.1208	0.1080
TCA	~ metab	-0.0090	0.4160
	~ metab + diet	0.1775	0.0238
	~ metab + diet + metab*diet	0.1252	0.1017
TCDCA	~ metab	-0.0042	0.3629
	~ metab + diet	0.1804	0.0226
	~ metab + diet + metab*diet	0.1287	0.0970
TLCA	~ metab	-0.0281	0.9000
	~ metab + diet	0.1612	0.0321
	~ metab + diet + metab*diet	0.1078	0.1284
TDCA	~ metab	-0.0253	0.7406
	~ metab + diet	0.1632	0.0309
	~ metab + diet + metab*diet	0.1371	0.0679
GCA	~ metab	-0.0184	0.5577
	~ metab + diet	0.1634	0.0308
	~ metab + diet + metab*diet	0.1125	0.1206
GCDCA	~ metab	0.0679	0.0653
	~ metab + diet	0.1819	0.0220
	~ metab + diet + metab*diet	0.1819	0.0220
GDCA	~ metab	0.0679	0.0653
	~ metab + diet	0.1819	0.0220
	~ metab + diet + metab*diet	0.1819	0.0220
GLCA	~ metab	-0.0212	0.6188
	~ metab + diet	0.1602	0.0327
	~ metab + diet + metab*diet	0.1867	0.0302
a_MCA	~ metab	-0.0283	0.9274
	~ metab + diet	0.1840	0.0211

	~ metab + diet + metab*diet	0.1332	0.0912
b_MCA	~ metab	-0.0134	0.4740
	~ metab + diet	0.1912	0.0184
	~ metab + diet + metab*diet	0.1525	0.0694
CA	~ metab	-0.0123	0.4575
	~ metab + diet	0.1677	0.0285
	~ metab + diet + metab*diet	0.1158	0.1154
CDCA	~ metab	0.0528	0.0916
	~ metab + diet	0.1602	0.0327
	~ metab + diet + metab*diet	0.1104	0.1241
UDCA	~ metab	-0.0255	0.7483
	~ metab + diet	0.1835	0.0213
	~ metab + diet + metab*diet	0.1312	0.0937
DCA	~ metab	0.0197	0.1977
	~ metab + diet	0.1628	0.0312
	~ metab + diet + metab*diet	0.1450	0.0599
LCA	~ metab	0.0259	0.1705
	~ metab + diet	0.1628	0.0312
	~ metab + diet + metab*diet	0.2009	0.0237

Short chain fatty acids

		R-squared	p-value
acetate	~ metab	-0.0250	0.6830
	~ metab + diet	0.1594	0.0389
	~ metab + diet + metab*diet	0.1020	0.1500
propinoate	~ metab	-0.0158	0.4974
	~ metab + diet	0.1654	0.0351
	~ metab + diet + metab*diet	0.1246	0.1135
butyrate	~ metab	-0.0198	0.5641
	~ metab + diet	0.1591	0.0391
	~ metab + diet + metab*diet	0.1017	0.1504

562

563

564 **References and Notes:**

565 1. F. C. Lessa, Y. Mu, W. M. Bamberg, Z. G. Beldavs, G. K. Dumyati, J. R. Dunn, M. M. Farley,
566 S. M. Holzbauer, J. I. Meek, E. C. Phipps, L. E. Wilson, L. G. Winston, J. A. Cohen, B. M.
567 Limbago, S. K. Fridkin, D. N. Gerding, L. C. McDonald, Burden of Clostridium difficile
568 infection in the United States, *N Engl J Med* **372**, 825–834 (2015).

569 2. D. A. Leffler, J. T. Lamont, Clostridium difficile infection, *N Engl J Med* **372**, 1539–1548
570 (2015).

571 3. G. N. Al-Rawahi, A. Al-Najjar, R. McDonald, R. J. Deyell, G. R. Golding, R. Brant, P. Tilley,
572 E. Thomas, S. R. Rassekh, A. O'Gorman, P. Wong, L. Turnham, S. Dobson, Pediatric oncology
573 and stem cell transplant patients with healthcare-associated Clostridium difficileinfection were
574 already colonized on admission, *Pediatr Blood Cancer* **353**, e27604–5 (2019).

575 4. E. J. Battaglioli, V. L. Hale, J. Chen, P. Jeraldo, C. Ruiz-Mojica, B. A. Schmidt, V. M.
576 Rekdal, L. M. Till, L. Huq, S. A. Smits, W. J. Moor, Y. Jones-Hall, T. Smyrk, S. Khanna, D. S.
577 Pardi, M. Grover, R. Patel, N. Chia, H. Nelson, J. L. Sonnenburg, G. Farrugia, P. C. Kashyap,
578 Clostridioides difficile uses amino acids associated with gut microbial dysbiosis in a subset of
579 patients with diarrhea, *Science Translational Medicine* **10**, eaam7019 (2018).

580 5. G. E. Bignardi, Risk factors for Clostridium difficile infection, *Journal of Hospital Infection*
581 **40**, 1–15 (1998).

582 6. R. Fekety, L. V. McFarland, C. M. Surawicz, R. N. Greenberg, G. W. Elmer, M. E. Mulligan,
583 Recurrent Clostridium difficile diarrhea: characteristics of and risk factors for patients enrolled in

584 a prospective, randomized, double-blinded trial, *Clinical Infectious Diseases* **24**, 324–333
585 (1997).

586 7. C. A. Lozupone, J. Stombaugh, A. Gonzalez, G. Ackermann, D. Wendel, Y. Vázquez-Baeza,
587 J. K. Jansson, J. I. Gordon, R. Knight, Meta-analyses of studies of the human microbiota,
588 *Genome Research* **23**, 1704–1714 (2013).

589 8. C. Staley, B. P. Vaughn, C. T. Graiziger, S. Singroy, M. J. Hamilton, D. Yao, C. Chen, A.
590 Khoruts, M. J. Sadowsky, Community dynamics drive punctuated engraftment of the fecal
591 microbiome following transplantation using freeze-dried, encapsulated fecal microbiota, *Gut*
592 *Microbes* **131**, 1–13 (2017).

593 9. C. Staley, C. R. Kelly, L. J. Brandt, A. Khoruts, M. J. Sadowsky, Complete Microbiota
594 Engraftment Is Not Essential for Recovery from Recurrent Clostridium difficileInfection
595 following Fecal Microbiota Transplantation, *mBio* **7**, e01965–16–9 (2016).

596 10. A. Weingarden, A. Gonzalez, Y. Vázquez-Baeza, S. Weiss, G. Humphry, D. Berg-Lyons, D.
597 Knights, T. Unno, A. Bobr, J. Kang, A. Khoruts, R. Knight, M. J. Sadowsky, Dynamic changes
598 in short- and long-term bacterial composition following fecal microbiota transplantation for
599 recurrent Clostridium difficile infection, *Microbiome* **3**, 10 (2015).

600 11. S. K. Dutta, M. Girotra, S. Garg, A. Dutta, E. C. von Rosenvinge, C. Maddox, Y. Song, J. G.
601 Bartlett, R. Vinayek, W. F. Fricke, Efficacy of Combined Jejunal and Colonic Fecal Microbiota
602 Transplantation for Recurrent Clostridium difficile Infection, *Clinical Gastroenterology and*
603 *Hepatology* **12**, 1–5 (2014).

12. J. R. Allegretti, S. Kearney, N. Li, E. Bogart, K. Bullock, G. K. Gerber, L. Bry, C. B. Clish, E. Alm, J. R. Korzenik, Recurrent Clostridium difficile infection associates with distinct bile acid and microbiome profiles, **43**, 1142–1153 (2016).

13. J. A. Sorg, A. L. Sonenshein, Bile salts and glycine as cogerminants for Clostridium difficile spores, *J. Bacteriol.* **190**, 2505–2512 (2008).

14. C. G. Buffie, V. Bucci, R. R. Stein, P. T. McKenney, L. Ling, A. Gobourne, D. No, H. Liu, M. Kinnebrew, A. Viale, E. Littmann, M. R. M. van den Brink, R. R. Jenq, Y. Taur, C. Sander, J. R. Cross, N. C. Toussaint, J. B. Xavier, E. G. Pamer, Precision microbiome reconstitution restores bile acid mediated resistance to Clostridium difficile, *Nature* **517**, 205–208 (2015).

15. A. J. Hryckowian, W. Van Treuren, S. A. Smits, N. M. Davis, J. O. Gardner, D. M. Bouley, J. L. Sonnenburg, Microbiota-accessible carbohydrates suppress Clostridium difficile infection in a murine model, *Nat Microbiol* **372**, 2369 (2018).

16. V. C. Antharam, E. C. Li, A. Ishmael, A. Sharma, V. Mai, K. H. Rand, G. P. Wang, Intestinal dysbiosis and depletion of butyrogenic bacteria in Clostridium difficile infection and nosocomial diarrhea, *Journal of Clinical Microbiology* **51**, 2884–2892 (2013).

17. S. Devkota, Y. Wang, M. W. Musch, V. Leone, H. Fehlner-Peach, A. Nadimpalli, D. A. Antonopoulos, B. Jabri, E. B. Chang, Dietary-fat-induced taurocholic acid promotes pathobiont expansion and colitis in Il10−/− mice, *Nature* **65**, 411–6 (2012).

18. X. Chen, K. Katchar, J. D. Goldsmith, N. Nanthakumar, A. Cheknis, D. N. Gerding, C. P. Kelly, A Mouse Model of Clostridium difficile–Associated Disease, *Gastroenterology* **135**, 1984–1992 (2008).

19. M. H. Sarafian, M. R. Lewis, A. Pechlivanis, S. Ralphs, M. J. W. McPhail, V. C. Patel, M.-E. Dumas, E. Holmes, J. K. Nicholson, Bile acid profiling and quantification in biofluids using ultra-performance liquid chromatography tandem mass spectrometry, *Anal. Chem.* **87**, 9662–9670 (2015).

20. B. Allen, M. Kon, Y. Bar-Yam, A new phylogenetic diversity measure generalizing the shannon index and its application to phyllostomid bats, *Am. Nat.* **174**, 236–243 (2009).

21. M. Kriss, K. Z. Hazleton, N. M. Nusbacher, C. G. Martin, C. A. Lozupone, Low diversity gut microbiota dysbiosis: drivers, functional implications and recovery, *Curr Opin Microbiol* **44**, 34–40 (2018).

22. M. G. I. Langille, J. Zaneveld, J. G. Caporaso, D. McDonald, D. Knights, J. A. Reyes, J. C. Clemente, D. E. Burkepile, R. L. Vega Thurber, R. Knight, R. G. Beiko, C. Huttenhower, Predictive functional profiling of microbial communities using 16S rRNA marker gene sequences, *Nature Biotechnology* **31**, 814–821 (2013).

23. J. M. Ridlon, D. J. Kang, P. B. Hylemon, Bile salt biotransformations by human intestinal bacteria, (2006).

24. M. Vital, A. C. Howe, J. M. Tiedje, Revealing the bacterial butyrate synthesis pathways by analyzing (meta)genomic data, *mBio* **5**, e00889–e00889–14 (2014).

25. M. Vital, J. Gao, M. Rizzo, T. Harrison, J. M. Tiedje, Diet is a major factor governing the fecal butyrate-producing community structure across Mammalia, Aves and Reptilia, *ISME J* **9**, 832–843 (2015).

645 26. N. Kumar, H. P. Browne, E. Viciani, S. C. Forster, S. Clare, K. Harcourt, M. D. Stares, G.
646 Dougan, D. J. Fairley, P. Roberts, M. Pirmohamed, M. R. J. Clokie, M. B. F. Jensen, K. R.
647 Hargreaves, M. Ip, L. H. Wieler, C. Seyboldt, T. Norén, T. V. Riley, E. J. Kuijper, B. W. Wren,
648 T. D. Lawley, Adaptation of host transmission cycle during Clostridium difficile speciation,
649 *Nature Genetics* **51**, 1315–1320 (2019).

650 27. T. L. Blankenship-Paris, B. J. Walton, Y. O. Hayes, J. Chang, Clostridium difficile infection
651 in hamsters fed an atherogenic diet, *Vet. Pathol.* **32**, 269–273 (1995).

652 28. T. L. Blankenship-Paris, J. Chang, F. G. Dalldorf, P. H. Gilligan, In vivo and in vitro studies
653 of Clostridium difficile-induced disease in hamsters fed an atherogenic, high-fat diet, *Lab. Anim.*
654 *Sci.* **45**, 47–53 (1995).

655 29. D. J. Cabral, S. Penumutchu, E. M. Reinhart, C. Zhang, B. J. Korry, J. I. Wurster, R. Nilson,
656 A. Guang, W. H. Sano, A. D. Rowan-Nash, H. Li, P. Belenky, Microbial Metabolism Modulates
657 Antibiotic Susceptibility within the Murine Gut Microbiome, *Cell Metabolism* **30**, 800–823.e7
658 (2019).

659 30. C. J. Kelly, L. Zheng, E. L. Campbell, B. Saeedi, C. C. Scholz, A. J. Bayless, K. E. Wilson,
660 L. E. Glover, D. J. Kominsky, A. Magnuson, T. L. Weir, S. F. Ehrentraut, C. Pickel, K. A. Kuhn,
661 J. M. Lanis, V. Nguyen, C. T. Taylor, S. P. Colgan, Crosstalk between Microbiota-Derived
662 Short-Chain Fatty Acids and Intestinal Epithelial HIF Augments Tissue Barrier Function, *Cell*
663 *Host Microbe* **17**, 662–671 (2015).

664 31. C. M. Cannon, J. S. Musuuza, A. K. Barker, M. Duster, M. B. Juckett, A. E. Pop-Vicas, N.
665 Safdar, Risk of Clostridium difficile Infection in Hematology-Oncology Patients Colonized With
666 Toxigenic C. difficile, *Infect Control Hosp Epidemiol* **38**, 718–720 (2017).

667 32. L. R. Thompson, J. G. Sanders, D. McDonald, A. Amir, J. Ladau, K. J. Locey, R. J. Prill, A.
668 Tripathi, S. M. Gibbons, G. Ackermann, J. A. Navas-Molina, S. Janssen, E. Kopylova, Y.
669 Vázquez-Baeza, A. Gonzalez, J. T. Morton, S. Mirarab, Z. Zech Xu, L. Jiang, M. F. Haroon, J.
670 Kanbar, Q. Zhu, S. Jin Song, T. Kosciolek, N. A. Bokulich, J. Lefler, C. J. Brislawn, G.
671 Humphrey, S. M. Owens, J. Hampton-Marcell, D. Berg-Lyons, V. McKenzie, N. Fierer, J. A.
672 Fuhrman, A. Clauset, R. L. Stevens, A. Shade, K. S. Pollard, K. D. Goodwin, J. K. Jansson, J. A.
673 Gilbert, R. Knight, Earth Microbiome Project Consortium, A communal catalogue reveals
674 Earth's multiscale microbial diversity, *Nature* **551**, 457–463 (2017).

675 33. E. Bolyen, J. R. Rideout, M. R. Dillon, N. A. Bokulich, C. C. Abnet, G. A. Al-Ghalith, H.
676 Alexander, E. J. Alm, M. Arumugam, F. Asnicar, Y. Bai, J. E. Bisanz, K. Bittinger, A. Brejnrod,
677 C. J. Brislawn, C. T. Brown, B. J. Callahan, A. M. Caraballo-Rodríguez, J. Chase, E. K. Cope, R.
678 Da Silva, C. Diener, P. C. Dorrestein, G. M. Douglas, D. M. Durall, C. Duvallet, C. F.
679 Edwardson, M. Ernst, M. Estaki, J. Fouquier, J. M. Gauglitz, S. M. Gibbons, D. L. Gibson, A.
680 Gonzalez, K. Gorlick, J. Guo, B. Hillmann, S. Holmes, H. Holste, C. Huttenhower, G. A.
681 Huttley, S. Janssen, A. K. Jarmusch, L. Jiang, B. D. Kaehler, K. B. Kang, C. R. Keefe, P. Keim,
682 S. T. Kelley, D. Knights, I. Koester, T. Kosciolek, J. Kreps, M. G. I. Langille, J. Lee, R. Ley, Y.-
683 X. Liu, E. Loftfield, C. Lozupone, M. Maher, C. Marotz, B. D. Martin, D. McDonald, L. J.
684 McIver, A. V. Melnik, J. L. Metcalf, S. C. Morgan, J. T. Morton, A. T. Naimey, J. A. Navas-
685 Molina, L. F. Nothias, S. B. Orchanian, T. Pearson, S. L. Peoples, D. Petras, M. L. Preuss, E.
686 Pruesse, L. B. Rasmussen, A. Rivers, M. S. Robeson, P. Rosenthal, N. Segata, M. Shaffer, A.

687 Shiffer, R. Sinha, S. J. Song, J. R. Spear, A. D. Swafford, L. R. Thompson, P. J. Torres, P. Trinh,
688 A. Tripathi, P. J. Turnbaugh, S. Ul-Hasan, J. J. J. van der Hooft, F. Vargas, Y. Vázquez-Baeza,
689 E. Vogtmann, M. von Hippel, W. Walters, Y. Wan, M. Wang, J. Warren, K. C. Weber, C. H. D.
690 Williamson, A. D. Willis, Z. Z. Xu, J. R. Zaneveld, Y. Zhang, Q. Zhu, R. Knight, J. G. Caporaso,
691 Reproducible, interactive, scalable and extensible microbiome data science using QIIME 2,
692 *Nature Biotechnology* **37**, 852–857 (2019).

693 34. B. J. Callahan, P. J. McMurdie, M. J. Rosen, A. W. Han, A. J. A. Johnson, S. P. Holmes,
694 DADA2: High-resolution sample inference from Illumina amplicon data, *Nat Meth* **13**, 581–583
695 (2016).

696 35. S. Janssen, D. McDonald, A. Gonzalez, J. A. Navas-Molina, L. Jiang, Z. Z. Xu, K. Winker,
697 D. M. Kado, E. Orwoll, M. Manary, S. Mirarab, R. Knight, N. Chia, Ed. Phylogenetic Placement
698 of Exact Amplicon Sequences Improves Associations with Clinical Information, *mSystems* **3**,
699 581 (2018).

700 36. Q. Wang, G. M. Garrity, J. M. Tiedje, J. R. Cole, Naive Bayesian classifier for rapid
701 assignment of rRNA sequences into the new bacterial taxonomy, *Appl. Environ. Microbiol.* **73**,
702 5261–5267 (2007).

703 37. C. Quast, E. Pruesse, P. Yilmaz, J. Gerken, T. Schweer, P. Yarza, J. Peplies, F. O. Glöckner,
704 The SILVA ribosomal RNA gene database project: improved data processing and web-based
705 tools, *Nucleic Acids Res* **41**, D590–6 (2013).

706 38. P. Yilmaz, L. W. Parfrey, P. Yarza, J. Gerken, E. Pruesse, C. Quast, T. Schweer, J. Peplies,
707 W. Ludwig, F. O. Glöckner, The SILVA and "All-species Living Tree Project (LTP)" taxonomic
708 frameworks, *Nucleic Acids Res* **42**, D643–8 (2014).

709 39. C. A. Lozupone, M. Hamady, S. T. Kelley, R. Knight, Quantitative and Qualitative
710 Diversity Measures Lead to Different Insights into Factors That Structure Microbial
711 Communities, *Appl. Environ. Microbiol.* **73**, 1576–1585 (2007).

712 40. Anaconda Software Distribution (available at https://anaconda.com).

713 41. L. Etienne-Mesmin, B. Chassaing, O. Adekunle, L. M. Mattei, F. D. Bushman, A. T.
714 Gewirtz, Toxin-positive Clostridium difficile latently infect mouse colonies and protect against
715 highly pathogenic C. difficile, *Gut* **67**, 860–871 (2018).

716 42. C. J. Kelly, E. E. Alexeev, L. Farb, T. W. Vickery, L. Zheng, C. Eric L, D. A. Kitzenberg, K.
717 D. Battista, D. J. Kominsky, C. E. Robertson, D. N. Frank, S. P. Stabler, S. P. Colgan, Oral
718 vitamin B12 supplement is delivered to the distal gut, altering the corrinoid profile and
719 selectively depleting Bacteroides in C57BL/6 mice, *Gut Microbes* **87**, 1–9 (2019).

720 43. H. Wickham, Tidyverse (available at https://CRAN.R-project.org/package=tidyverse).

721 44. A. Kassambara, M. Kosinski, P. Biecek, S. Fabian, survminer: Drawing Survival Curves
722 using "ggplot2" (available at http://www.sthda.com/english/rpkgs/survminer/).

723 45. T. M. Therneau, T. Lumley, survival: Survival Analysis (available at
724 https://github.com/therneau/survival).

725 46. H. Wickham, *ggplot2* (Springer, 2010).

726 47. C. Ahlmann-Eltze, ggsignif: Significance Brackets for “ggplot2” (available at
727 https://github.com/const-ae/ggsignif).

728 48. C. O. Wilke, cowplot: Streamlined Plot Theme and Plot Annotations for “ggplot2” (available
729 at https://wilkelab.org/cowplot).

730 49. A. Gonzalez, J. A. Navas-Molina, T. Kosciolek, D. McDonald, Y. Vázquez-Baeza, G.
731 Ackermann, J. DeReus, S. Janssen, A. D. Swafford, S. B. Orchanian, J. G. Sanders, J.
732 Shorenstein, H. Holste, S. Petrus, A. Robbins-Pianka, C. J. Brislawn, M. Wang, J. R. Rideout, E.
733 Bolyen, M. Dillon, J. G. Caporaso, P. C. Dorrestein, R. Knight, Qiita: rapid, web-enabled
734 microbiome meta-analysis, *Nature* **15**, 796–798 (2018).

735

Acknowledgments: We would like to thank Jordi Lanis and Sean Colgan for advice on the employed CDI mouse model and Sally Stabler for her assistance in measuring SCFAs. **Funding:** We would like to thank the University of Colorado Department of Medicine's Outstanding Early Career Science Award for supporting this work as well as support to Keith Hazleton from the Institutional Training Grant for Pediatric Gastroenterology from NIDDK (5T32-DK067009-12) and Clinical Fellow Awards from the Cystic Fibrosis Foundation (HAZLET18DO and HAZLET19DO). Kathleen Arnolds was supported by T32-AI007405 Training Program in Immunology. High performance computing was supported by a cluster at the University of Colorado Boulder funded by National Institutes of Health 1S10OD012300. **Author contributions:** KH conceived of and conducted experiments, analyzed data and wrote the paper; CM analyzed sequence data and made figures; KA generated and analyzed data from qPCR experiments and toxin ELISA; NN generated 16S rRNA sequence and qPCR data and aided in analysis and results interpretation; NMH aided in mouse experiments, 16S rRNA sequencing and generated data from toxin ELISA; NR and MAworked with KH to develop a novel bile acid panel and aided in analysis and interpretation of results, CL directed and contributed to all aspects of the project. All authors contributed to the manuscript. **Competing interests:** The authors declare no competing financial interests. **Data and materials availability:** The 16S rRNA has been deposited in QIITA ***(49)***(Qiita Study ID: 12849) and at EBI (pending)